[^{13}C]bicarbonate kinetics in humans: intra- vs. interindividual variations

CHARLES S. IRVING, WILLIAM W. WONG, ROBERT J. SHULMAN, E. O'BRIAN SMITH, AND PETER D. KLEIN
USDA/ARS Children's Nutrition Research Center, Department of Pediatrics, Baylor College of Medicine, Houston, Texas 77030

IRVING, CHARLES S., WILLIAM W. WONG, ROBERT J. SHULMAN, E. O'BRIAN SMITH, AND PETER D. KLEIN. *[^{13}C]bicarbonate kinetics in humans: intra- vs. interindividual variations.* Am. J. Physiol. 245 (Regulatory Integrative Comp. Physiol. 14): R190–R202, 1983.—A comprehensive multicompartmental analysis of HCO_3^- kinetics was carried out on five normal, resting, fasted adults on three separate occasions at 1-wk to 1-mo intervals to obtain a set of bicarbonate kinetic parameters and estimates of their inter- and intraindividual variations for use in the design and analysis of future nutrient oxidation studies. Following a rapid bolus of $NaH^{13}CO_3$ (10 $\mu mol \cdot kg^{-1}$ iv), the decay of ^{13}C enrichment of breath CO_2 could be described by a three-exponential decay process and a linearly time-dependent term that accounted for changes in the ^{13}C enrichment of metabolic fuels. The data were fitted subsequently to a mammillary multicompartmental model that consisted of a central pool and two peripheral pools of 3,310, 3,490, and 8,070 $\mu mol \cdot kg^{-1}$ HCO_3^--CO_2. Labeled CO_2 was eliminated from the central pool by respiratory and nonrespiratory routes at rates of 101 and 97 $\mu mol \cdot kg^{-1} \cdot min^{-1}$, respectively. The within-subject and among-subject variances were similar for the amount of freely exchangeable bicarbonate (14,870 $\mu mol \cdot kg^{-1}$), CO_2 output (101 $\mu mol \cdot kg^{-1} \cdot min^{-1}$), bicarbonate flux (198 $\mu mol \cdot kg^{-1} \cdot min^{-1}$), and the fraction of administered bicarbonate recovered in breath (0.51). Comparison of variances associated with the assignment of a population mean value to a new subject and the variance associated with the use of a value obtained in the same individual on another day indicated that there was no advantage to making a determination on an alternate day over using a population value. Efforts should be made to compile population values for bicarbonate kinetics in different age groups and metabolic, nutritional, and pathological states for use in interpretation of nutrient oxidation data.

compartmental modeling; pool sizes; turnover rates; nutrient oxidation

THE INVESTIGATOR WHO WISHES to determine the utilization and oxidation of nutrients in humans by employing ^{13}C-labeled compounds faces a choice of two options. He may elect to determine whole-body flux and overall oxidation rates from primed constant-infusion experiments. The benefit of such studies is that they do not require precisely timed sample collection: they require only the isotopic enrichment of the nutrient at plateau, values for CO_2 production and for the total recovery of labeled bicarbonate. Moreover nutrient flux and oxidation can be calculated by simple algebraic methods readily available in any laboratory. The fundamental limitation to this option is that the interpretation of changes in whole-body flux, oxidation, and utilization often is limited by their global nature, which prevents further stipulation of nutrient pool sizes and the sites of oxidation within the subject. Such data can be obtained in humans only from the alternative method, which employs multicompartmental analysis of data collected after administration of a bolus dose. Such methods have been used in earlier nutrient oxidation studies in animals (31, 34) and humans (12, 18, 32, 35, 36) when ^{14}C was employed, but are only now being adopted by those investigators using ^{13}C.

Bicarbonate pool sizes and kinetic parameters are essential components of multicompartmental analysis of nutrient oxidation. They are required to account for the effect of transit through the bicarbonate pools on the rate of appearance of labeled carbon in breath and to quantitate the total recovery of labeled respiratory CO_2. Earlier tracer studies of bicarbonate kinetics (1–3, 7–10, 13–18, 21, 23, 30, 31, 34–37) that were a part of ^{14}C nutrient oxidation studies have left a variety of bicarbonate models in the literature, and this may confound the investigator who needs to incorporate such kinetic treatment into his analysis of nutrient oxidation. We undertook a series of studies of bicarbonate kinetics in humans to obtain a unified model that can be incorporated into multicompartmental analyses of nutrient absorption, utilization, and oxidation. We present here the details of the model and compare it with previous models and to a composite model based on physiological and anatomical data. We also report an analysis of intra- and interindividual variations in bicarbonate kinetic parameters. This analysis shows that a single set of bicarbonate parameters matched to the appropriate subject population can be used in place of values determined in the same individual on an alternate day to the one used for nutrient oxidation measurements. The unified bicarbonate model also provides a framework for future studies of the effects of age, nutritional and metabolic status, exercise, and acidosis on bicarbonate kinetic parameters.

METHODS

Materials. $NaH^{13}CO_3$ (Merck Sharp and Dohme Canada, Montreal, Quebec), containing 90 atom% excess

(APE) ^{13}C as assayed by gas isotope ratio mass spectrometry, was made up at a concentration of 200 mM in saline and sterilized by filtration. A second solution having five times the concentration (1 M) was also prepared for a single study. Both solutions were tested for sterility and absence of pyrogens before use.

The concentrations and isotopic enrichment of $NaH^{13}CO_3$ in the solutions used for administration of labeled bicarbonate were verified in the following manner. A known aliquot (60 or 100 μl) of the $NaH^{13}CO_3$ solution was added to 1.0 ml of 55 mM Na_2CO_3 solution. Approximately 0.5 ml of the $NaHCO_3$-Na_2CO_3 mixture was transferred into one of the reservoirs of a gas conversion Y tube containing 1.0 ml of 100% H_3PO_4 in the other reservoir. After freezing the $NaHCO_3$-Na_2CO_3 mixture with a methanol-dry ice bath, the Y tube was evacuated to less than 5 μm via a high-vacuum system. The Y tube was disconnected from the high-vacuum system. After thawing, the Y tube was tilted and the mixture was allowed to react with the 100% H_3PO_4 for several hours in a water bath at 25°C. The CO_2 released from the solution was purified and transferred to a sample bulb via a high-vacuum system for mass spectrometry. The isotopic ratio of the $NaH^{13}CO_3$ (R_{sample}) is given by $(R_{mix} - NR_{standard})/(1 - N)$, where R_{mix} and $R_{standard}$ are the ^{13}C isotopic ratios of the mixture and Na_2CO_3 standard, respectively, and N is the mole fraction of CO_2 derived from Na_2CO_3. R_{sample} was 90 ± 7 APE ^{13}C on the basis of six determinations. The concentration of bicarbonate in the $NaH^{13}CO_3$ solutions was verified manometrically by the amount of CO_2 generated by addition of H_3PO_4 as described above.

Subjects. The five volunteers described in Table 1 were recruited from the Texas Medical Center personnel. All had normal medical histories and were free from any metabolic abnormalities. Informed written consent was obtained from each in accord with the Helsinki Agreement, and the protocol was approved by the Baylor Institutional Review Board for Human Research.

Protocol. Bicarbonate kinetics were determined in each subject on three occasions separated by intervals of 1 wk to 1 mo. Individual determinations are identified by subject (*1–5*) and trial (*A*, *B*, or *C*). *Subject 5* underwent an additional study in which he received a 30-fold larger dose of $NaH^{13}CO_3$. Each subject was admitted to the Clinical Research Center of Texas Children's Hospital the night before the study. No food was permitted after 9 P.M., and the subject remained in the fasted state, confined to his or her room, with minimal physical activity for the duration of the protocol. The subject was fitted and acquainted with the use of a face mask (no. 4 or 5, Laerdal, Armonk, NY) equipped with two one-way valves (DHD 235A, DHD Medical Products, Canastoga, NY). The inlet valve was connected to a Wright respirometer (RM 121, Fraser Hulake, Orcano Park, NJ) and the outlet valve was attached to a plastic 3-liter sampling bag (no. 1740, lot 1908712, Hudson Oxygen Therapy Sales, Temecula, CA).

TABLE 1. *Anthropometric data on subjects studied*

Subj No.	Sex	Age, yr	Ht, cm	Wt, kg	BSA, m^2
1	M	23	185	80	2.028
2	F	22	168	55	1.596
3	F	21	156	53	1.519
4	M	31	170	70	1.825
5	F	28	164	48	1.472

BSA, body surface area.

At approximately 8 A.M., the subject put on the face mask and base-line samples of respiratory CO_2 were taken for isotopic abundance. Three timed respiratory volumes were measured using the Wright respirometer, and samples of expired air were collected for subsequent measurement of CO_2 concentration by gas chromatography. Similar respiratory measurements were made at 60, 120, 180, 240, and 300 min after the start of the protocol. After samples for respiratory $^{13}CO_2$ abundance had been obtained at −30, −15, and −1 min, each subject received a bolus injection of 10 μmol·kg^{-1} of $NaH^{13}CO_3$ (0.05 ml solution·kg^{-1}) and breath samples were collected over approximately 30 s at 1, 3, 5, 7, 9, 12, 15, 20, 30, 45, 60, 90, 120, 150, 180, 240, 300, and 360 min for isotopic abundance measurements. In the additional study of *subject 4*, who received 300 μmol·kg^{-1} $NaH^{13}CO_3$, expiratory CO_2 samples were collected for an additional 4 h at hourly intervals.

Analytical procedures. The CO_2 concentration (%CO_2 ATPD) of breath samples taken during the respiratory volume measurements was analyzed by gas-solid chromatography on a Carle III instrument (Carle Instruments, Anaheim, CA) at a temperature of 150°C and an argon carrier gas flow of 20 ml/min using a 3 mm × 2 m stainless steel column packed with 60/80 mesh Carbosphere (Alltech, no. 5680).

CO_2 analysis for ^{13}C-^{12}C abundance was measured in the automatic gas isotope ratio mass spectrometer, based on a 3–60 Sectorr magnet sector instrument (Nuclide Corporation, State College, PA) previously described (28). The isotopic abundances were corrected for ^{17}O, ^{18}O, instrument background, abundance sensitivity, and valve leakage (22).

Data analysis. Data analysis and modeling were performed on an IBM 370 computer (Argonne National Laboratory, Argonne, IL) using SPEAKEZ (Speakeasy Computer, Chicago, IL) and the Simulation Analysis and Modeling (SAAM-27) program (4), modified to run interactively in Conversational Monitoring System (CMS). Graphic output was obtained using the Tellagraf program (Integrated Software Systems, San Diego, CA). The three programs were run interactively using CMS EXEC routines, which facilitated the transfer of data sets among the programs.

CO_2 output. For each hourly respiratory measurement, three respiratory volumes, corrected for temperature and pressure, were averaged and multiplied by their %CO_2 to obtain an estimate of CO_2 output (μmol·min^{-1}), which was normalized using the subject's weight (μmol·kg^{-1}·min^{-1}) or body surface area (μmol·m^2·min^{-1}) derived from the subject's height and weight (5). CO_2 output for the entire 6-h kinetic measurement was obtained by averaging the hourly values. This average CO_2 output value was used in subsequent calculations.

Determination of breath $^{13}CO_2$. ^{13}C abundance of breath CO_2 was calculated from mass spectrometric ratiometry

values as previously described (27) and expressed as δ‰ vs. the limestone standard, PDB. Incremental changes in ^{13}C abundance over base-line values (δ‰ over base line, DOB) were obtained by subtracting the mean of δ‰ vs. PDB at −30 and −15 min from the subsequent δ‰ vs. PDB values. Analytical standard deviations of DOB values were obtained from the standard deviations of three gas isotope ratiometry measurements of δ‰ vs. PDB.

Analysis of $^{13}CO_2$ data has been carried out using δ‰ units, rather than atom% excess units (APE), which might be more familiar to investigators who work with the isotopic enrichments of organic molecules determined by gas chromatography-mass spectrometry (GCMS) ratiometry. The changes in isotopic enrichments measured by gas isotope ratiometry usually are 1,000-fold smaller than those routinely measured by GCMS isotope ratiometry. A difference of 1 δ‰ unit is equivalent to 1.123×10^{-3} APE units, making APE an inconveniently large unit to use to measure small differences in the isotopic composition of gases, such as CO_2. The use of APE units for breath CO_2 enrichments would hinder comparisons to variations of basal enrichments of breath CO_2 and to natural ^{13}C enrichments of metabolic fuels, both of which are reported in δ‰ units. Furthermore δ‰ units are always used for instrument performance and calibration. For physiological applications, δ‰ units can be converted easily to percent dose recoveries or to moles of excess $^{13}CO_2$ for comparison to plasma levels of ^{13}C-labeled nutrients and their metabolites.

Multiexponential analysis of DOB decay curves. In the initial examination of the data, the DOB decay curves were fitted to a three-exponential decay function using the SAAM-27 program (model code 1). Accelerated and decelerated rates of decay were observed in several curves after 240 min, when isotopic enrichments were in the range of 1–4 DOB units. Large coefficients of variations were obtained when these curves were fitted to a three-exponential decay function. This problem could be overcome either by excluding from analysis all data collected after 240 min or by adding an additional term to the three-exponential function that would account for the terminal behavior of the decay curves. The accelerated and decelerated change in isotopic abundance of respiratory CO_2 probably results from changes during a fast in the fractional utilization of different metabolic fuels of different ^{13}C isotopic composition (29). The maximum drift in the basal ^{13}C enrichment observed was 1.8 DOB units, which is small compared with the range of the isotopic enrichments of carbohydrates and fats and the shifts that have been observed on switching metabolic fuels (29). The direction of base-line drift is determined by ^{13}C isotopic enrichment of the recently ingested meal compared with the ^{13}C enrichment of glycogen and fat stores. If the enrichment of the last meal is greater than the stores, then a negative drift will occur. Rather than excluding breath $^{13}CO_2$ enrichment data obtained beyond 240 min, we chose to quantitate the magnitude of drift in the basal ^{13}C enrichment of breath CO_2 by introducing an additional term into the three-exponential decay function.

When those curves with decelerated terminal decays were tested for adherence to a four-exponential decay function, the best-fit value of the fourth exponential term was forced to zero, indicating that the appropriate decay function consisted of three exponentials and a nonexponential (linear or constant) term. The DOB curves were fitted to functions consisting of three exponential decay terms plus either a constant term (*Eq. 1*) or a linear time-dependent term (*Eq. 2*)

$$\mathrm{DOB}_t = A_1 e^{-\lambda_1 t} + A_2 e^{-\lambda_2 t} + A_3 e^{-\lambda_3 t} + K \qquad (1)$$

$$\mathrm{DOB}_t = A_1{}^{-\lambda_1 t} + A_2 e^{-\lambda_2 t} + A_3 e + K \cdot t \qquad (2)$$

The best fits were obtained when the time-dependent term was incorporated (*Eq. 2*). Curves that showed an accelerated rate of fall in DOB after 240 min also could be fitted with ease to *Eq. 2*; in these instances the linear term assumed a negative value. Subsequently all the DOB decay curves were fitted to this decay function in which the linear term accounted for either positive or negative drift in the base-line value of δ‰ vs. PDB over the 6 h of the kinetic measurements. The nonlinear least-squares regression analysis by the SAAM-27 program provided best-fit values and standard deviations for the preexponential coefficient (A), exponential (λ), and linear (K) terms. It should be noted that deceleration in the terminal rate of decay might in some cases result from the presence of a fourth exponential decay process and not from base-line drift. Information on a fourth exponential term is lost when the curves are corrected by a positive base-line drift term (K).

When the analytical standard deviations for gas isotope ratiometry were entered into the SAAM-27 program along with the DOB values, the variance of the data based on the initial difference between the observed and calculated values was more than 100 times greater than the variance of the data estimated from the analytical standard deviations, which prevented adjustments of the estimated parameters by iteration. This indicated that variance of physiological origin exceeded that of the analytical method. To overcome this problem and to accommodate a wide range of possible best-fit values for the estimated parameters, multiexponential analysis was carried out in three sequential stages using fractional standard deviation (FSD) values of 0.20, 0.05, and 0.01. The analysis began with a set of best-guess values, and the best-fit values of the estimated parameters obtained at each stage were used as the initial values in the next stage. The standard deviations for the estimated parameters to be reported are given for FSD = 0.01, unless otherwise noted. The interactive operation of this analysis was carried out automatically, using a CMS EXEC routine. The area under the DOB decay curves (AUC), corrected for base-line drift, was calculated using *Eq. 3*

$$\mathrm{AUC} = \sum_{i=1}^{n} \frac{Ai}{i} \qquad (3)$$

Compartmental analysis. The DOB decay curves, corrected for base-line drift, were fitted by the SAAM-27 program (model code 10) to the three-compartment mammillary model shown in Fig. 1. The model consisted of a central pool (*compartment 1*) that was in relatively

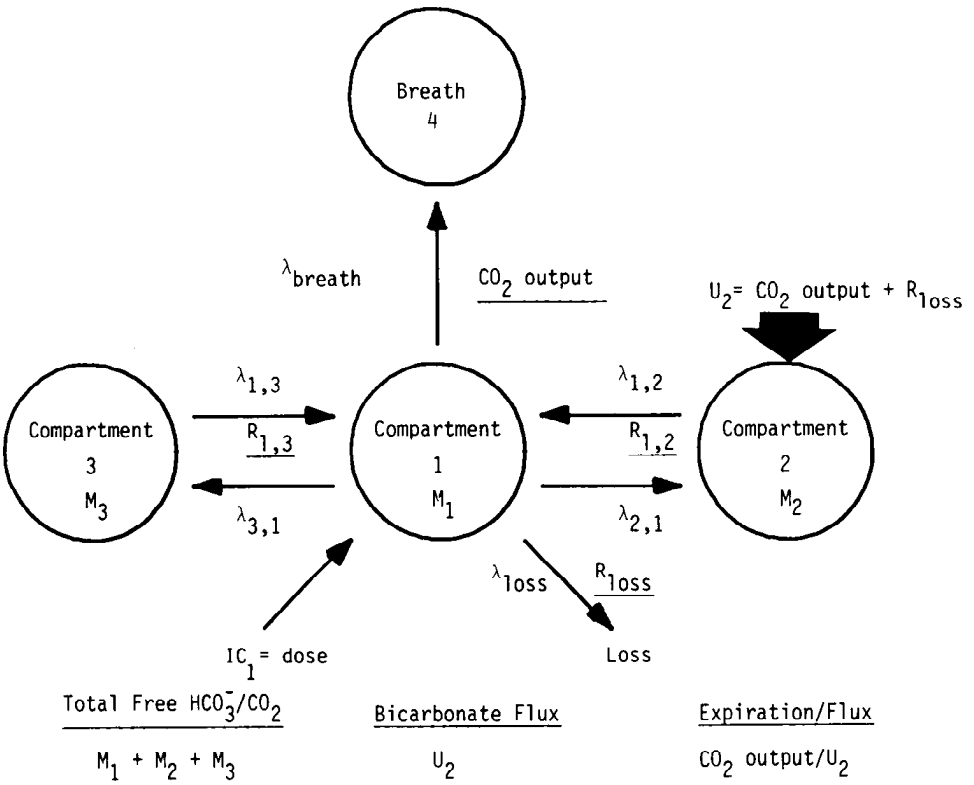

FIG. 1. Bicarbonate compartmental model and definitions of bicarbonate kinetic parameters: fractional rate constants (λ, min^{-1}), pool sizes (M, $\mu mol \cdot kg^{-1}$), transfer rates (R, $\mu mol \cdot kg^{-1} \cdot min^{-1}$), endogenous input ($U_2$, $\mu mol \cdot kg^{-1} \cdot min^{-1}$), and CO_2 output ($\mu mol \cdot kg^{-1} \cdot min^{-1}$).

rapid equilibrium with one peripheral pool (*compartment 2*) and in relatively slower equilibrium with a second peripheral pool (*compartment 3*). The intravenous bolus of labeled bicarbonate was introduced into the central compartment, and labeled bicarbonate and CO_2 were treated as the same tracer substance. Labeled breath CO_2 was regarded as being derived from the central compartment and was collected in a breath compartment (*compartment 4*). The contents of the breath compartment were emptied 0.25 min before sample collection. The amount of tracer that had accumulated in the breath compartment (M_4, $\mu mol \cdot kg^{-1}$) over 0.25 min was converted to ^{13}C abundance using *Eq. 4*

$$DOB = \left(\frac{M_4 \cdot 4}{\dot{V}CO_2 \cdot R_{PDB}}\right) \cdot 1{,}000 \qquad (4)$$

where R_{PDB} is the ^{13}C abundance of the Pee Dee belemnite standard (0.0112373) and $\dot{V}CO_2$ is CO_2 output expressed in $\mu mol \cdot kg^{-1} \cdot min^{-1}$. The model also contained a nonrespiratory elimination pathway from the central compartment that had to be introduced to account for the relatively rapid rate of decay of breath ^{13}C abundance. In the steady-state solution, endogenous unlabeled CO_2 was introduced into *compartment 2* and was equal to the amount of CO_2 lost by respiratory and nonrespiratory pathways. Fractional rate constants (λ_{ij}), pool sizes, (M_i), and transfer rates (R_{ij}) for the compartment model were computed from corrected DOB decay curves and CO_2 output data, as previously described for the exponential terms, in three stages using successive FSD of 0.2, 0.05, and 0.01. In each iteration, the best values obtained were used as initial estimates for the next stage and the steady-state solutions were calculated after the final stage had been completed. In addition to analysis of individual decay curves, compartmental analysis was also carried out on a DOB curve obtained by averaging the 15 additional curves.

Statistical analysis. The variance (σ_{pop}) associated with estimating a parameter (X_{ij}) for the *subject i* on *day j* from the mean value of the parameter ($X_{..}$) obtained for the appropriate population is given by *Eq. 5*

$$(\sigma_{pop})^2 = \sigma_A{}^2 + \sigma^2 \qquad (5)$$

where $\sigma_A{}^2$ is the among-subject variance for the estimation of the mean value for *subject i* (X_i) from $X_{..}$ and σ^2 is the within-subject variance for the estimation of the value of *day j* (X_{ij}) from X_i. The variance $(\sigma_{ind})^2$ associated with estimating a parameter X_{ij} from another value of X_{ij}, obtained in the same individual on an alternate *day j'*, is given by

$$(\sigma_{ind})^2 = 2\sigma^2 \qquad (6)$$

The values of $\sigma_A{}^2$ and σ^2 for bicarbonate kinetic parameters were determined (27) from the data collected for the three trials in five subjects, using *Eqs. 7* and *8*, for analysis of variance of a random-effects model (33)

$$\sigma^2 = \frac{\sum_{i=1}^{a} \sum_{j=1}^{n} (X_{ij} - \bar{X}_i)^2}{a(n-1)} \qquad (7)$$

$$\sigma_A{}^2 = \left[\frac{n \sum_{i=1}^{a} (\bar{X}_i - \bar{X}_{..})}{(a-1)} \cdot \sigma^2\right] \cdot n^{-1} \qquad (8)$$

where a and n are the number of subjects and trials,

respectively, and X_i and $X_{..}$ are given by

$$\bar{X}_i = \sum_{j=1}^{n} \frac{X_{ij}}{n} \quad (9)$$

and

$$\bar{X}_{..} = \sum_{i=1}^{a} \bar{X}_i/a \quad (10)$$

Since within-subject variances (σ) were large compared with the variances associated with the regression analyses and analytical errors, corrections for the latter were not carried out.

RESULTS

Decay of breath $^{13}CO_2$. Breath $^{13}CO_2$ levels following administration of $NaH^{13}CO_3$ (10 μmol·kg^{-1} iv) are given in the APPENDIX (Table A1) for the three trials of all five subjects. The uncorrected breath $^{13}CO_2$ decay curves are shown in Fig. 2. The six exponential decay parameters and the base-line drift term obtained by fitting the decay curves to *Eq. 2* are tabulated in Table 2 for all trials within all subjects. The significant improvement in the fit of the $^{13}CO_2$ curves that results from the inclusion of the base-line drift term is shown in Fig. 3. An example of positive and negative base-line drift in the same subject is shown in Fig. 4, along with the significant reduction of within-subject variation that results from base-line drift corrections. The areas under the decay curves extrapolated to infinite time given in Table 2 were determined from the multiexponential parameters using *Eq. 3*. These values were used in combination with CO_2 output data (Table 2) and dose levels to obtain the estimated percent dose recovery given in Table 2. The average values of CO_2 output and percent dose recovery for all trials in all subjects were 101 μmol·kg^{-1}·min^{-1} and 51.7%, respectively.

In an attempt to detect additional decay terms that might have gone undetected during the 6-h period of measurements due to the low ^{13}C enrichment of the terminal breath samples, a 30-fold greater dose of $NaH^{13}CO_3$ (300 μmol·kg^{-1}) was administered to *subject 4* and breath collections were made for 10 h (Fig. 5). At the termination of the measurements, the DOB value was 6.34 ± 0.08‰, indicating that the ^{13}C enrichment was high enough and the accuracy of analysis sensitive enough to reflect the existence of additional exponential terms in the decay process, if such were present. No evidence was found for more than three decay processes over 10 h following administration of $NaH^{13}CO_3$. Variations in the decay curve between 6 and 10 h far exceeded the analytical error and must have been of physiological origin. The three exponential decay terms obtained by fitting the decay curve to *Eq. 2*, and listed in Fig. 6, were in excellent agreement with the mean values obtained from *subject 4* given in Table 2.

The possibility that a significant percent of the intravenous dose of $NaH^{13}CO_3$ could have been excreted on the first passage through the lungs was considered. Since sampling began at 1 min after administration of the bolus, such losses would have to take place in the interval between injection and the first breath collection time point. In a fifth measurement on *subject 4*, a rapid bolus of $NaH^{13}CO_3$ (10 μmol·kg^{-1}) was administered and breath samples were collected at 0.3, 0.5, 0.8, and 1 min following injection. The maximum rate of $^{13}CO_2$ excretion occurred at 0.5 min, and the total percent dose recovered over the 1st min was 3.67%. The triangulation process of integration between the zero-time and 1-min values would have accounted for most of this dose recov-

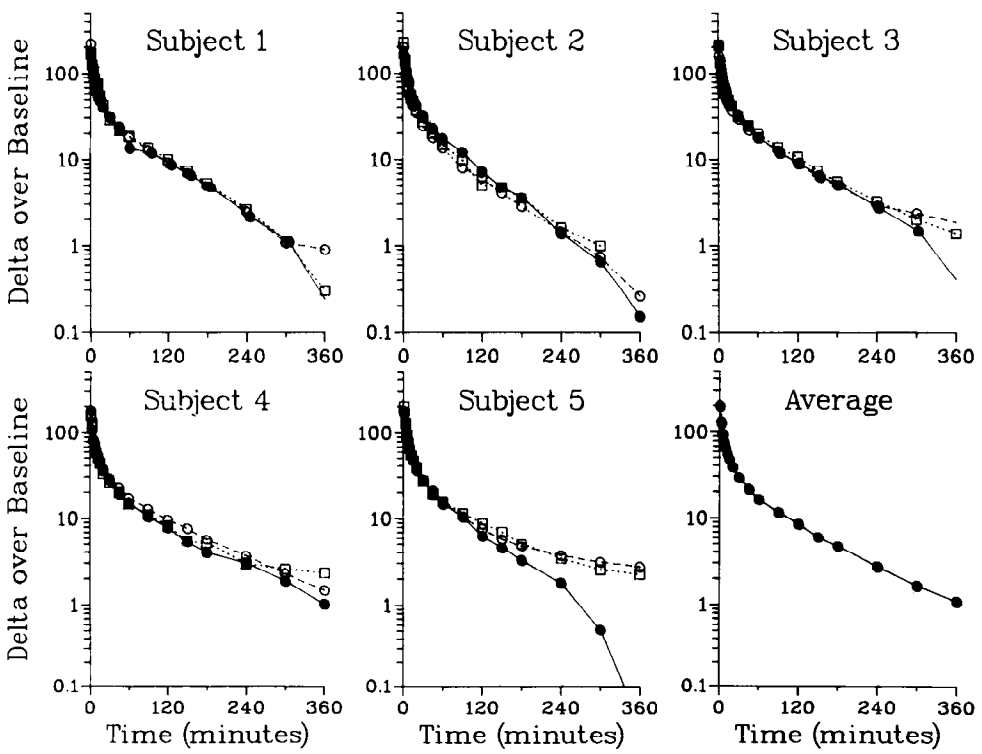

FIG. 2. ^{13}C enrichment decay curves (DOB vs. time) of breath CO_2 after administration of $NaH^{13}CO_3$ (10 μmol·kg^{-1} iv) to *subjs 1–5* over *trials A* (●), *B* (○), and *C* (□).

TABLE 2. *Preexponential, exponential, and linear term values obtained in $^{13}CO_2$ isotope decay curves following intravenous bolus injection of $NaH^{13}CO_2$ together with CO_2 production values and percent dose recovered*

Subj No.	Trial	A_1	A_2	A_3	λ_1	λ_2	λ_3	K	AUC, δ·min	$\dot{V}CO_2$, $\mu mol \cdot kg^{-1} \cdot min^{-1}$	% Dose
1	A	98.00	73.13	26.20	0.2258	0.0701	0.009	−0.0022	4,394	83	45.53
		±6.19	±6.69	±0.38	±0.0172	±0.0038	±0.00009	±0.00005		±16	
	B	202.56	61.94	41.86	0.5016	0.1154	0.0130	0.0012	4,157	117	60.73
		±13.36	±13.03	±1.12	±0.0563	±0.0189	±0.0002	±0.0001		±22	
	C	1,332.1	120.24	32.60	1.7905	0.1004	0.0098	−0.0018	5,266	118	77.58
		±182.66	±1.88	±0.31	±0.1413	±0.0017	±0.00007	±0.00004		±30	
Mean ± SD		544.22	85.10	33.55	0.8393	0.0953	0.0106	−0.0009	4,606	106	61.28
		±684.33	±30.94	±7.88	±0.8352	±0.0230	±0.0021	±0.0018	±584	±19.93	±16.03
2	A	117.92	26.95	29.70	0.1628	0.0341	0.0121	−0.0006	3,972	87.4	43.34
		±2.83	±2.54	±1.11	±0.0067	±0.0038	±0.0002	±0.00003		±15	
	B	189.56	44.70	19.15	0.3275	0.0464	0.0103	−0.0006	3,399	104	44.13
		±3.05	±1.12	±0.45	±0.0073	±0.0014	±0.0001	±0.00003		±9	
	C	196.39	54.59	24.72	0.3271	0.0536	0.0118	0.0009	3,708	114	52.79
		±3.66	±1.97	±0.65	±0.0101	±0.0023	±0.0002	±0.00009		±10.0	
Mean ± SD		167.96	42.08	24.52	0.2725	0.0447	0.0114	−0.0001	3,693	101.8	46.75
		±43.47	±14.00	±5.28	±0.0950	±0.0098	±0.001	±0.0009	±286	±13.44	±5.24
3	A	173.28	61.67	23.33	0.3468	0.0482	0.0079	−0.0026	4,743	108	63.97
		±3.44	±1.52	±0.46	±0.0107	±0.0014	±0.0001	±0.00009		±8	
	B	135.58	25.19	33.49	0.2470	0.0554	0.0115	0.0036	3,915	78.5	38.37
		±3.21	±2.80	±0.87	±0.0089	±0.0066	±0.0002	±0.00009		±5	
	C	163.68	69.83	36.18	0.4213	0.0868	0.0107	0.0016	4,583	96	54.94
		±4.61	±3.97	±0.48	±0.0214	±0.0042	±0.0001	±0.00007		±12	
Mean ± SD		157.51	52.23	31.00	0.3384	0.0635	0.0100	0.0009	4,414	94.17	52.42
		±19.59	±23.77	±6.78	±0.0874	±0.0205	±0.0019	±0.0032	±439	±14.84	±12.98
4	A	157.38	46.17	13.22	0.3363	0.0343	0.0060	−0.0014	4,017	93.3	46.80
		±2.86	±0.74	±0.54	±0.0081	±0.001	±0.0002	±0.0002		±7	
	B	105.46	65.83	27.90	0.3989	0.0743	0.0089	0.0009	4,299	75.8	40.69
		±3.35	±2.79	±0.42	±0.0237	±0.0029	±0.0001	±0.0001		±8	
	C	125.16	36.15	28.51	0.2359	0.0681	0.0014	0.0051	3,569	102	45.45
		±4.47	±4.58	±0.71	±0.0109	±0.0067	±0.0002	±0.0001		±10	
Mean ± SD		129.33	49.38	23.21	0.3237	0.0589	0.0087	0.0015	3,962	90.37	44.32
		±26.21	±15.10	±8.66	±0.0822	±0.0216	±0.0027	±0.0033	±368	±13.34	±3.21
5	A	121.22	61.29	26.04	0.3093	0.0659	0.0112	−0.0012	3,645	121	55.07
		±3.15	±2.74	±0.36	±0.0140	±0.0024	±0.00008	±0.00002		±10	
	B	137.62	40.49	14.58	0.2230	0.0314	0.0075	0.0049	3,847	112	53.80
		±2.05	±1.04	±1.27	±0.0055	±0.0016	±0.0005	±0.0003		±9	
	C	150.42	84.20	28.03	0.4809	0.0863	0.0102	0.0042	4,023	106	53.25
		±4.57	±2.98	±0.42	±0.0254	±0.0028	±0.0001	±0.0001		±6	
Mean ± SD		136.42	61.99	22.88	0.3377	0.0612	0.0097	0.0026	3,838	113	54.04
		±14.64	±21.87	±7.26	±0.1313	±0.0278	±0.0019	±0.0033	±189	±7.55	±0.94
Total mean ± SD		227.09	58.16	27.03	0.4223	0.0647	0.0101	0.0007	4,103	101.07	51.76
		±79.59	±7.45	±2.20	±0.1049	±0.0083	±0.0004	±0.0006	±174	±4.06	±2.97

$\dot{V}CO_2$, CO_2 output; AVC, area under the curve; A, λ, and K, preexponential, exponential and linear terms, respectively.

ery in the absence of the short collection intervals.

Multicompartmental analysis. Breath $^{13}CO_2$ enrichment decay curves corrected for base-line drift were fitted to the compartmental model shown in Fig. 1. Pool sizes, fractional rate constants, and transfer rates obtained from the analysis of the decay curve averaged over all 15 measurements are given in Fig. 6. The compartmental model of bicarbonate kinetics in normal fasting adults consisted of a central pool (*compartment 1*) of 3,310 $\mu mol \cdot kg^{-1}$ with a half-life of 2.6 min that exchanged at the rapid rate of 667 $\mu mol \cdot kg^{-1} \cdot min^{-1}$ with a pool (*compartment 2*) of equal size, 3,490 $\mu mol \cdot kg^{-1}$. At the same time, the central pool exchanged more slowly (210 $\mu mol \cdot kg^{-1} \cdot min^{-1}$) with a larger pool (*compartment 3*) containing 8,070 $\mu mol \cdot kg^{-1}$. Using a value of 24 mM for the concentration of circulating bicarbonate, the apparent volume of the central pool is 134 $ml \cdot kg^{-1}$. The smaller peripheral pool, whose half-life is 3.6 min was ascribed to rapidly perfused tissues such as liver, intestine, heart, and brain. The larger peripheral pool, whose half-life was 26 min, was assigned to more slowly perfused tissues such as muscle and skin. Labeled CO_2 was eliminated from the central pool by respiratory and nonrespiratory routes at rates of 101 and 97 $\mu mol \cdot kg^{-1} \cdot min^{-1}$, respectively. Together, the three compartments comprised a pool of freely exchangeable bicarbonate of 14,870 $\mu mol \cdot kg^{-1}$ with a half-life of 52 min that turned over at a rate of 198 $\mu mol \cdot kg^{-1} \cdot min^{-1}$. CO_2 excretion accounted for only 50.1% of the flux of the freely exchangeable bicarbonate.

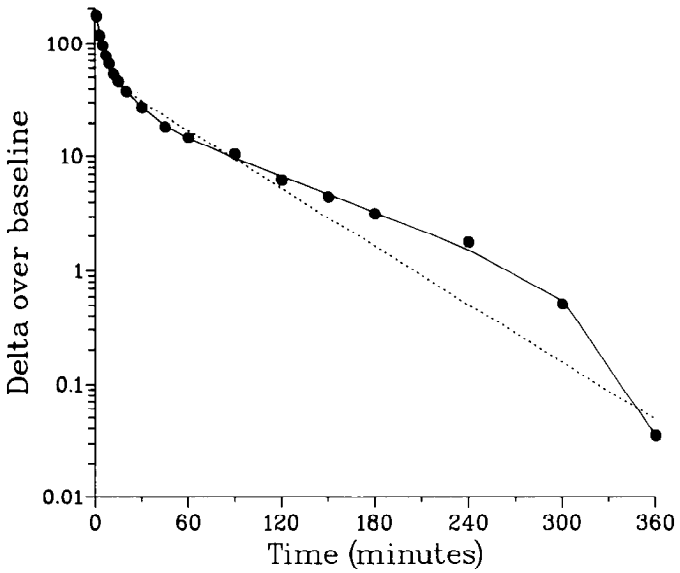

FIG. 3. ^{13}C enrichment decay curve of breath CO_2 for *subj 5, trial A* (●), best fit to 3-exponential decay function (----) given by *Eq. 1*, and best fit to 3-exponential linear-term decay function (—) given by *Eq. 2*.

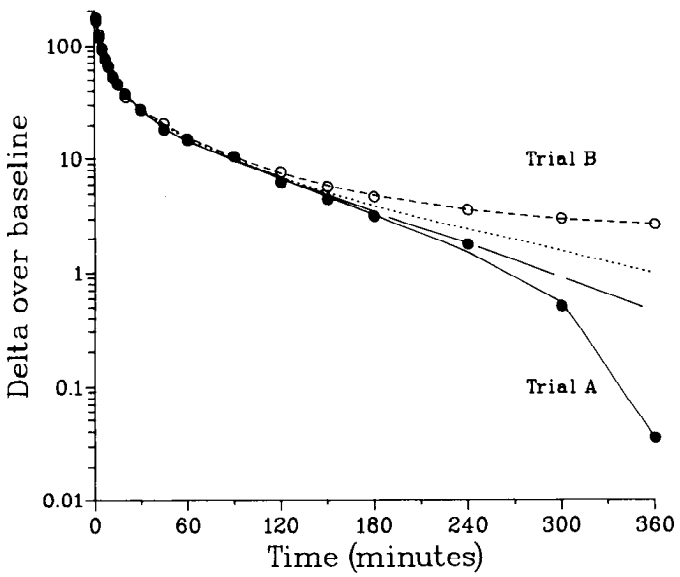

FIG. 4. ^{13}C enrichment decay curve of breath CO_2 for *subj 5, trials A* (●) and *B* (○), best-fit curves using *Eq. 2* for *trials A* (—) and *B* (--), and curves corrected for base-line drift for *trials A* (——) and *B* (-----).

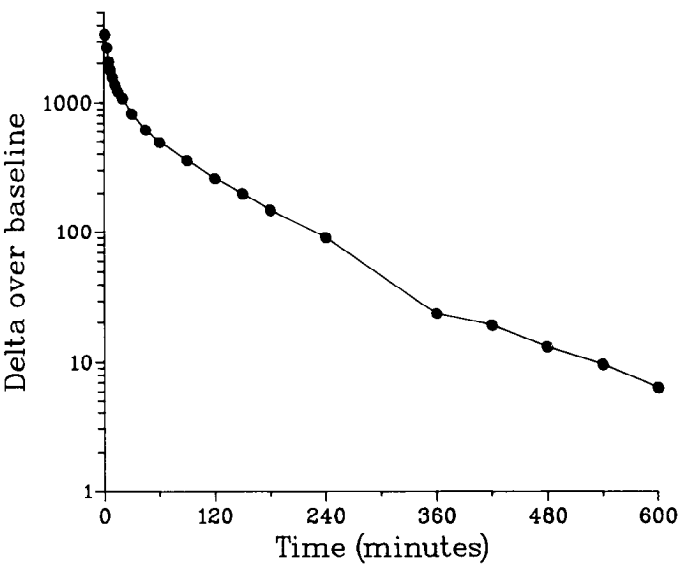

FIG. 5. ^{13}C enrichment decay curve of breath CO_2 after administration of $NaH^{13}CO_3$ (300 $\mu mol \cdot kg^{-1}$ iv) to *subj 4* (●). Parameters for fit of *Eq. 2* are $A_1 = 2{,}103 \pm 64$, $A_2 = 1{,}189 \pm 52$, $A_3 = 810 \pm 8$, $\lambda_1 = 0.322 \pm 0.018$, $\lambda_2 = 0.0576 \pm 0.0024$, $\lambda_3 = 0.00958 \pm 0.00004$, and $K = 0.00724 \pm 0.00014$.

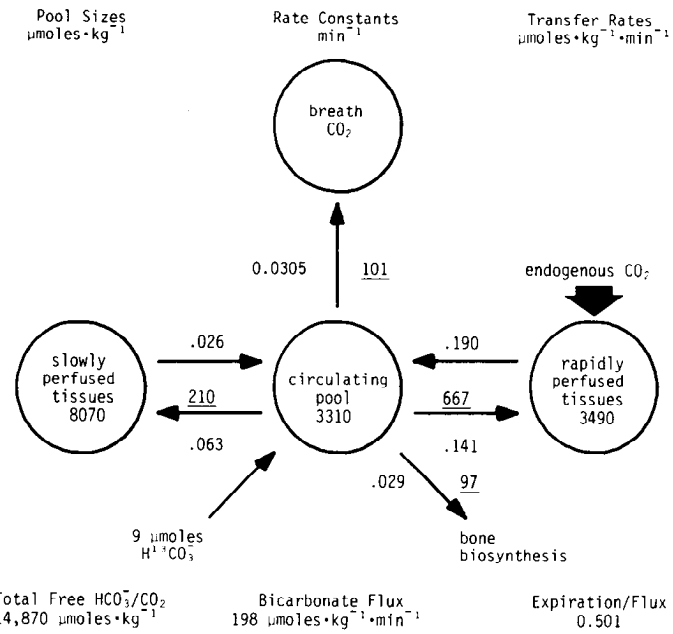

FIG. 6. Bicarbonate compartmental model derived from averaged DOB decay curve. See Fig. 1 for definition of kinetic parameters.

The fractional rate constants, pool sizes, and transfer rates for all trials in all subjects are given in Tables 3 and 4. Among the bicarbonate pools, the central pool varied the least in size, whereas the size of the rapidly perfused tissue pool (*compartment 2*) fluctuated the most as judged by the standard deviations over all 15 measurements. Fractional rate constants and transfer rates for respiratory output of CO_2 were the least variable kinetic parameters, whereas the fractional rate constant for the transfer of bicarbonate from the central pool to the rapidly perfused tissue pool was the most variable. The mean values for parameters given in Table 4 are in good agreement with the parameters obtained from analysis of the averaged DOB curve (Fig. 6).

Inter- and intraindividual variations. The [^{13}C]bicarbonate kinetic parameters that are of use in the design and analysis of substrate oxidation measurements, i.e., the amount of freely exchangeable bicarbonate (M_{free}), CO_2 output, bicarbonate flux (Q), and the fraction of administered bicarbonate recovered in breath (F), were subjected to a random-effects model analysis of variance. Table 5 gives the values obtained for within-subject variance (σ) and among-subject variance (σ_A). For all four bicarbonate parameters, the within-subject variance was larger than the among-subject variance. Another measure of relative benefits of alternative experimental designs can be obtained from variance (σ_{pop}) associated

TABLE 3. *Fractional rate constants for bicarbonate kinetics in 3 trials of 5 subjects*

Subj No.	Trial	λ_{21}	λ_{12}	λ_{31}	λ_{13}	λ_{loss}	λ_{breath}
		$min^{-1} \cdot 10^4$					
1	A	448 ± 33	1,480 ± 132	457 ± 14	221 ± 3	240 ± 2	199 ± 2
	B	1,634 ± 169	2,225 ± 305	1,161 ± 116	431 ± 19	284 ± 9	428 ± 14
	C	2,499 ± 930	6,972 ± 1,637	679 ± 49	288 ± 6	157 ± 9	328 ± 21
Mean ± SD		1,527 ± 1,029	3,559 ± 2,979	772 ± 351	313 ± 107	227 ± 64	318 ± 114
2	A	565 ± 20	6,574 ± 40	140 ± 20	216 ± 10	246 ± 02	186 ± 2
	B	1,386 ± 36	1,113 ± 30	399 ± 13	186 ± 2	408 ± 4	318 ± 3
	C	1,215 ± 36	1,172 ± 39	388 ± 14	215 ± 3	340 ± 3	373 ± 4
Mean ± SD		1,055 ± 432	980 ± 281	309 ± 146	205 ± 17	331 ± 81	292 ± 96
3	A	1,441 ± 50	1,419 ± 47	437 ± 12	1,728 ± 2	193 ± 2	337 ± 4
	B	834 ± 45	1,052 ± 80	491 ± 54	324 ± 14	301 ± 3	186 ± 2
	C	1,392 ± 81	2,094 ± 133	794 ± 30	321 ± 5	259 ± 4	312 ± 5
Mean ± SD		1,223 ± 336	1,521 ± 527	574 ± 192	272 ± 86	251 ± 54	278 ± 80
4	A	1,625 ± 91	1,126 ± 53	337 ± 17	113 ± 4	287 ± 7	245 ± 6
	B	1,250 ± 85	2,177 ± 143	597 ± 20	260 ± 4	267 ± 4	182 ± 2
	C	611 ± 34	1,130 ± 107	548 ± 33	294 ± 7	286 ± 3	236 ± 2
Mean ± SD		1,161 ± 512	1,478 ± 605	494 ± 138	222 ± 96	280 ± 11	221 ± 34
5	A	929 ± 48	1,541 ± 83	449 ± 15	244 ± 3	252 ± 3	305 ± 4
	B	940 ± 26	855 ± 26	232 ± 8	130 ± 3	230 ± 2	264 ± 2
	C	1,609 ± 106	2,505 ± 145	738 ± 23	266 ± 3	297 ± 5	334 ± 5
Mean ± SD		1,160 ± 389	1,643 ± 829	473 ± 253	213 ± 72	260 ± 34	301 ± 34
Total mean ± SD		1,225 ± 530	1,834 ± 1,523	524 ± 249	245 ± 81	270 ± 59	282 ± 75

λ, fractional rate constant.

TABLE 4. *Bicarbonate pool sizes and transfer rates in 3 trials of 5 subjects*

Subj No.	Trial	M_1	M_2	M_3	M_{free}	$R_{1,2}$	$R_{1,3}$	R_{loss}
		$\mu mol \cdot kg^{-1}$				$\mu mol \cdot kg^{-1} \cdot min^{-1}$		
1	A	4,161 ± 49	2,498 ± 196	8,951 ± 106	15,612	369 ± 12	198 ± 5	100.1 ± 0.4
	B	2,731 ± 92	2,881 ± 408	7,357 ± 337	12,969	641 ± 35	317 ± 27	77.7 ± 1.0
	C	3,590 ± 254	1,537 ± 193	8,472 ± 115	13,600	1,072 ± 301	243 ± 7	56.5 ± 0.9
Mean ± SD		3,494 ± 719	2,305 ± 692	8,260 ± 818	14,060 ± 1,380	694 ± 354	253 ± 60	78.1 ± 21.8
2	A	4,694 ± 45	7,125 ± 455	3,955 ± 392	14,876	468 ± 8	66 ± 9	115.4 ± 0.5
	B	3,261 ± 40	6,194 ± 148	6,991 ± 112	16,447	689 ± 8	130 ± 4	133.3 ± 0.6
	C	3,052 ± 38	5,024 ± 147	5,509 ± 104	13,586	589 ± 8	118 ± 4	103.9 ± 0.6
Mean ± SD		3,669 ± 893	6,114 ± 1,052	5,185 ± 1,987	14,970 ± 1,432	582 ± 110	104 ± 34	117.5 ± 14.8
3	A	3,199 ± 42	4,446 ± 105	8,109 ± 93	15,755	630 ± 12	140 ± 3	61.8 ± 0.4
	B	4,208 ± 49	5,289 ± 573	6,377 ± 443	15,755	630 ± 12	206 ± 22	127.0 ± 0.5
	C	3,071 ± 49	2,882 ± 137	7,585 ± 116	13,539	603 ± 19	243 ± 7	79.5 ± 0.4
Mean ± SD		3,493 ± 622	4,206 ± 1,221	7,357 ± 888	15,057 ± 1,315	597 ± 37	196 ± 52	89.4 ± 33.6
4	A	3,748 ± 100	7,182 ± 299	11,200 ± 244	22,132	809 ± 22	126 ± 5	107.7 ± 1.0
	B	4,160 ± 65	3,246 ± 133	9,550 ± 114	16,957	707 ± 29	248 ± 6	111.2 ± 0.4
	C	4,316 ± 49	4,333 ± 425	8,028 ± 274	16,679	489 ± 13	236 ± 13	123.8 ± 0.5
Mean ± SD		4,074 ± 293	4,921 ± 2,032	9,592 ± 1,586	18,589 ± 3,071	668 ± 162	203 ± 67	114.2 ± 8.4
5	A	3,958 ± 52	3,820 ± 156	7,281 ± 114	15,060	588 ± 15	117 ± 5	99.8 ± 0.5
	B	4,229 ± 45	7,096 ± 174	7,547 ± 110	18,874	607 ± 8	98 ± 3	97.3 ± 0.5
	C	3,172 ± 55	2,837 ± 92	8,799 ± 81	14,819	711 ± 26	234 ± 4	94.5 ± 0.5
Mean ± SD		3,786 ± 548	4,585 ± 2,230	7,876 ± 810	16,248 ± 2,277	635 ± 65	170 ± 68	97.2 ± 2.6
Total mean ± SD		3,703 ± 590	4,426 ± 1,839	7,654 ± 1,856	15,785 ± 2,350	635 ± 161	185 ± 70	99.3 ± 22.5

M, pool size; *R*, transfer rate.

with the assignment of the population value to a new subject and the variance (σ_{ind}) associated with the use of a value obtained in the same individual on another day. Comparison of σ_{pop} with σ_{ind} indicated that for all parameters the uncertainty associated with the use of an appropriate population value was less than the uncertainty associated with values obtained on an alternate day in the same subject.

DISCUSSION

There are a variety of multiexponential and multicompartmental descriptions of bicarbonate kinetics in ani-

TABLE 5. *Mean values and statistical measures of total free bicarbonate pool, CO_2 output, flux, and recovery within individuals and among the group*

	M_{free}, $\mu mol \cdot kg^{-1}$	$\dot{V}CO_2$, $\mu mol \cdot kg^{-1} \cdot min^{-1}$	Q, $\mu mol \cdot kg^{-1} \cdot min^{-1}$	F
Mean	15,785	101	200	0.51
σ	2,015	14	16	0.08
σ_A	1,307	4	13	0.03
σ_{ind}	2,850	20	220	0.11
σ_{pop}	2,402	15	21	0.09

M, free pool size; $\dot{V}CO_2$, CO_2 output; Q, flux; F, fractional total recovery. $Q = \dot{V}CO_2 + R_{loss}$. $F = \dot{V}CO_2/Q$.

TABLE 6. *Exponential constants describing the decay of labeled CO_2 in breath following intravenous bolus of labeled bicarbonate*

Species	Length of Measurement, min	min^{-1} λ_1	λ_2	λ_3	Ref.
Human	0–360	0.3237	0.0589	0.0087	This work*
	0–360			0.0097	3
	0–360			0.0089	19
	0–160	0.32	0.0139		30
	0–120	0.134	0.0107		36
	0–480	0.041	0.0113	0.00072	14
Cat	0–300	0.243	0.0234	0.0012	16
Dog	0–120	0.315	0.0729	0.0118	8
Rat	0–120	0.93	0.16	0.025	31
	0–180	0.227	0.090	0.016	23

λ, exponential constant. *Derived from averaged DOB curve.

mals and humans in the literature. This can lead to confusion when one attempts to incorporate bicarbonate kinetics into estimates of the rate and extent of nutrient and drug oxidations. In the following sections a unified description of bicarbonate kinetics will be presented, based on a review of published bicarbonate kinetic parameters and a comparison of the data obtained in these studies.

Bicarbonate kinetics as a multiexponential process. The exponential decay constants obtained in this study are compared with previously reported values in Table 6. The terminal decay constant of 0.0087 min^{-1} obtained for normal resting adults in this study is in excellent agreement with the values given by Baker et al. (3) and Manougian and co-workers (19) who studied the disappearance of $^{14}CO_2$ in breath over 6 h following a bolus dose of $NaH^{14}CO_3$. Segal et al. (30) and Winchell et al. (36) carried out measurements over shorter times and found larger terminal decay rates whose values fell between those of the second and the terminal decay constants obtained in this study. Issekutz et al. (14) resolved the curves of the fraction of bicarbonate remaining to be excreted into three exponential processes, of which the terminal decay rate was much longer than any such process previously reported. This long terminal decay process, whose half-life was 478 min, was not observed during the 10-h study we carried out using a large dose of $NaH^{13}CO_3$. A comparison of the decay constants obtained in this study with those obtained by Coxon and Robinson (8) in the dog and by Morris and Morgan-Simpson (23) in the rat (in both instances over 120 min) suggests that bicarbonate kinetics in these animals and in humans might be determined by similar physiological processes. Coxon and Robinson noted that the decay curves for $^{14}CO_2$, ^{22}Na, and ^2H_2O were similar despite their different chemical properties and suggested that their rates of transfer were determined by the rate of blood flow per unit mass tissue.

Bicarbonate kinetics as a multicompartmental process. Two types of bicarbonate models have been described in the literature. The first consists of a three-compartment mammillary model with respiratory elimination from the central compartment, initially described by Steele (34) and subsequently adopted by Shipley et al. (31), Waterhouse et al. (35), and Malmendier et al. (18). The second is a two-compartment model with respiratory and nonrespiratory losses from the first miscible pool described by Fowle et al. (12) and later by Winchell et al. (36). The bicarbonate pool sizes and transfer rates obtained in this study are compared with previously reported values in Table 7. When pool sizes and fractional turnover rates reported for the Steele-type model (34) are compared with our values, it is seen that the absence of nonrespiratory losses of labeled CO_2 leads to greater sequestration of bicarbonate in the slowly turning over pool. In this respect, the Steele model is qualitatively different from the model derived in this study. On the other hand, the sizes of the first miscible pool reported for the Fowle-Winchell model are in good agreement with the combined pool sizes of *compartments 1* and *2* obtained in this study. The pool size of *compartment 3* in this study is identical to the size of the peripheral pool reported by Winchell et al. (36). Moreover the model derived herein is identical to the one used by Winchell with the important distinction that the central pool in the Fowle-Winchell model has been resolved into a central pool and a pool of rapidly perfused tissue. The model derived in this study can be termed a "unified" model, because it incorporates the three compartments of the Steele-type model and the irreversible loss of the Fowle-Winchell model.

Postulated anatomical and physiological identities of bicarbonate compartments and transfer processes. Steele (34) assigned the central bicarbonate compartment in the cat to circulating blood, the peripheral compartment with rapid turnover to bicarbonate in soft tissue, and the peripheral pool with slow turnover to the solid bicarbonate of bone. Shipley et al. (31) assigned the central pool in the rat to extracellular bicarbonate, the rapidly turning over peripheral pool to intracellular bicarbonate, and the slowly exchanging pool to a combination of bone bicarbonate and organic carbon such as acetoacetate, oxaloacetate, or malate. No anatomical assignment of the two peripheral pools in the Steele-type model was made in previous studies in humans (18, 35). Turning to the two-compartment model, Fowle et al. (12) divided the system into extracellular and intracellular spaces and assigned the nonrespiratory loss of CO_2 to the exchange of CO_2 with a very large and slowly exchanging pool such as bone bicarbonate. They argued that equilibration across capillary membranes is much faster than transport across membranes separating intracellular from extracellular fluid. On the other hand, Winchell and co-

TABLE 7. *HCO_3^--CO_2 pool sizes and fractional rate constants*

mmol·kg^{-1}				min^{-1}						Ref.
M_1	M_2	M_3	M_{total}	λ_{21}	λ_{12}	λ_{31}	λ_{13}	λ_{resp}	λ_{loss}	
3.3	3.5	8.1	14.9	0.190	0.141	0.063	0.26	0.031	0.029	This work*
5.475	3.5		9.0	0.093	0.15			0.022	0.017	12
5.48	7.88		13.36	0.067	0.046			0.027	0.005	36
6.12	8.01		14.12	0.063	0.043			0.024	0.005	32
2.485	1.88	10.7	15.1	0.16	0.23	0.19	0.048	0.057		18
1.06	4.31†	10.1†	15.44†	0.508	0.125	0.095	0.010	0.103		35

M, pool size; λ, fractional rate constant. *Derived from averaged DOB curve. †Estimated from λ values.

workers (36) showed that the equilibration of blood CO_2 with tissue is membrane independent and is determined by blood perfusion rates. This allowed them to assign the first pool to blood and to tissues with a high ratio of perfusion compared with CO_2-HCO_3^- content (e.g., abdominal and thoracic viscera) and the second pool to tissues with low ratios of perfusion to bicarbonate content (e.g., resting skeletal muscle). Nonrespiratory losses from the first pool were ascribed to fixation in bone or losses in urine or sweat. Fahri and Rahn (11) calculated the rate of change of CO_2 stores of various tissues in humans and found that the heart, brain, and "other" compartments responded rapidly to changes in levels of circulating CO_2, whereas muscle responded more slowly.

Construction of a composite model of bicarbonate kinetics in humans from physiological data. Comparison of the mathematically derived multicompartmental model obtained from tracer kinetic data with a composite model assembled from published physiological and anatomical data can aid in the identification of bicarbonate pools and transfer processes. A composite model of bicarbonate kinetics can be constructed from the estimates of arterial and venous CO_2 levels, tissue production rates and levels of bicarbonate and CO_2, and organ blood flow rates. To construct such a model *1*) organs are grouped into compartments according to their rates of CO_2 uptake and release; *2*) the sizes of the HCO_3^--CO_2 compartments are calculated from the tissue levels of HCO_3^--CO_2; *3*) fractional turnover rates are determined from arterial and venous CO_2 levels, tissue blood flow, and CO_2 production rates, assuming complete single-pass mixing of tissue and vascular HCO_3^--CO_2; and *4*) the fractional rate constant for exchange of circulating bicarbonate with the sink of bone bicarbonate is estimated from blood HCO_3^--CO_2 levels, skeletal blood flow rate, and the extraction ratio of bicarbonate from blood by bone. Such a physiological bicarbonate model is shown in Fig. 7, which was constructed from the blood flow rate, HCO_3^--CO_2 organ levels, and CO_2 storage data compiled by Fahri and Rahn (11). The model consists of three pools of freely exchangeable bicarbonate: a central vascular pool (2,111 μmol·kg^{-1}), a heart-brain-"other" pool (2,389 μmol·kg^{-1}), and a muscle pool (6,122 μmol·kg^{-1}). CO_2 production from the heart-brain-"other" pool and the muscle pool were 127.5 and 25.5 μmol·kg^{-1}·min^{-1}, respectively, which yielded a rate of CO_2 output of 153 μmol·kg^{-1}·min^{-1}. The vascular bicarbonate exchanges with the large sink of bone bicarbonate (72,066 μmol·kg^{-1}) at a rate of 23.9 μmol·kg^{-1}·min^{-1}. The latter value was estimated using skeletal blood flow rate equal to 5% of the cardiac output and a 30% extraction ratio of bicarbonate between bone and blood (26). The total flux of freely exchangeable bicarbonate is 176.9 μmol·kg^{-1}·min^{-1} of which 86.5% is accounted for by respiratory losses.

Comparison of multicompartmental and composite models. The amount of freely exchangeable bicarbonate in the composite model (10,586 μmol·kg^{-1}) estimated from the tissue levels is less than the freely exchangeable bicarbonate found in this study (15,000 μmol·kg^{-1}) and that obtained from previous tracer studies (Table 7). The distribution of free bicarbonate among the three pools in the composite model and the compartmental model obtained in this study is in good agreement. The fractional rate constants for exchange of bicarbonate with the fast and slow peripheral pools in the compartmental model were 30 and 50% less, respectively, than those obtained from the composite model for which complete single-pass exchange of vascular and tissue bicarbonate was assumed. The smaller fractional rate constants for the compartmental model suggest that the assumption of complete HCO_3^--CO_2 exchange between the vascular and tissue compartments is incorrect. This is further substantiated by the fact that the reduction in fractional rate constants found in the compartmental model is in excellent agreement with the transcapillary exchange rates of 35–58% calculated by Coxon and Robinson (8) from femoral arteriovenous ratios of specific activity of blood CO_2 in dogs after injection of [^{14}C]bicarbonate.

The fraction of bicarbonate flux attributable to exchange between the freely exchangeable bicarbonate and the sink of bone bicarbonate was 0.868 in the physiological model and is not of sufficient magnitude to explain the recovery of only 50% of tracer bicarbonate obtained in this study. The reported percent dose recoveries found in breath CO_2 by other workers are shown in Table 8 and range from 42 to 85%. Nonrespiratory losses of labeled bicarbonate have been ascribed to exchange with bone bicarbonate, exchange with metabolic intermediates, and/or large respiratory losses before sampling began (10, 12, 30, 35). The composite model indicates that exchange with bone bicarbonate can account for only one-third of the nonrespiratory losses found in this study, and it is unlikely that this exchange rate would have undergone a threefold increase under normal physiological conditions in our subjects. Large respiratory losses of labeled CO_2 in the first minute following intravenous injection of labeled bicarbonate did not occur in our studies, during which time the cumulative percent dose excretion of labeled CO_2 was only 3.6%. Biosynthetic incorporation of labeled bicarbonate and exchange of

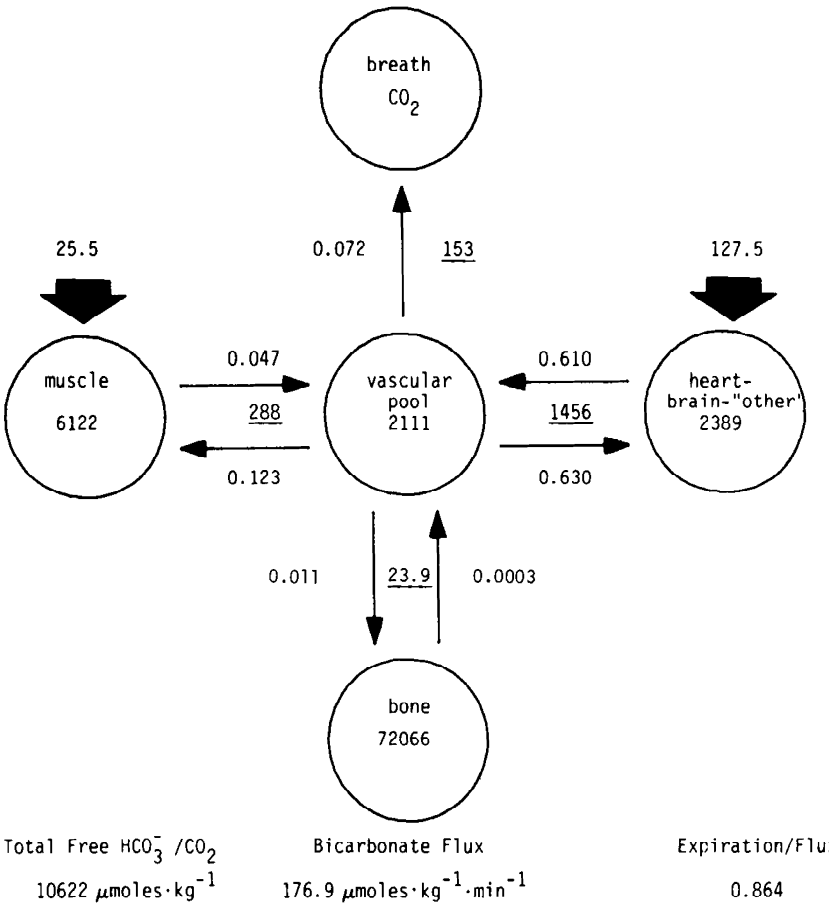

FIG. 7. Composite bicarbonate compartmental model. Kinetic parameters as defined in Figs. 1 and 6.

TABLE 8. *Comparison of percent dose recovery of labeled CO_2 in breath*

Species	Method of Administration	Time of Recovery, min	Dose Recovered, %	$\dot{V}_{CO_2}$, μmol·kg^{-1}·min^{-1}	Ref.
Human	Bolus	Infinite	51	101	This work
	Bolus	0–480	80	115	14
	Constant infusion	0–600	80		15
	Constant infusion	0–2,880	88–93		13
	Primed constant infusion	0–120	81		1
	Bolus	Infinite	56.4	116	12
	Bolus	Infinite	84.3	145.6	36
	Bolus	0–120	70	118	35
Rat	Bolus	0–120	42–53		31
Cat	Bolus	0–300	79–81		16

labeled CO_2 with labile carboxyl groups such as those of oxaloacetate (6) appear to be the most reasonable explanations of nonrespiratory losses of labeled bicarbonate in our study.

The production of endogenous CO_2 within *compartment 2* (Fig. 1) used in steady-state solution of the multicompartmental model is in agreement with the major part of CO_2 production occurring in the heart-brain-"other" pool of the composite model. When the bicarbonate model is incorporated into nutrient oxidation studies, $^{13}CO_2$ generated by oxidation of labeled nutrients in tissues with low levels of carbonic anhydrase would have to be converted to $H^{13}CO_3^-$ by erythrocytes and should be introduced directly into the central bicarbonate pool.

Implications for the design of nutrient oxidation studies. Calculation of the percent of ^{13}C-labeled nutrient that has undergone oxidation in a human subject is carried out by dividing the percent dose of the labeled nutrient that is recovered in breath as $^{13}CO_2$ by the fraction of an intravenous dose of $NaH^{13}CO_3$ that can be recovered as breath $^{13}CO_2$. The value that has been used most widely for this fractional recovery term is 0.81, which was derived from the ratio of the output of $^{14}CO_2$ in breath to the rate of infusion of $NaH^{14}CO_3$ after plateau had been reached in constant-infusion experiments (13–15). It has been assumed (20, 24, 25) that the same fractional recovery of bicarbonate will be obtained in other metabolic, nutritional, and pathological states. However, the value of 0.51 obtained in this study indicates that it is more reasonable to expect that the fractional recovery of bicarbonate can change. The range over which the values can change and the factors leading to the changes are not known at present. Prudence dictates that nutrient oxidation measurements be coupled with bicarbonate kinetic determinations under the particular protocol being studied. This can be achieved at present by either *1*) determining an average set of bicarbonate kinetic parameters for the appropriate population and applying these values to additional subjects in similar metabolic, nutritional, and pathological states, or *2*) determining the bicarbonate kinetic parameters in each subject and applying them to nutrient oxidation studies carried out

on alternate days. The large degree of intraindividual variation found for these parameters indicates that the effort required to determine bicarbonate kinetics on alternate days in every subject undergoing nutrient oxidation studies is not justified at present. Instead, efforts should be made to establish population values for bicarbonate kinetics in different age groups, metabolic and nutritional states, and pathological conditions likely to be of interest in nutrient oxidation protocols. The bicarbonate kinetic parameters reported here are appropriate population values for one such group: normal, overnight-rested, fasted adult subjects.

Ideally bicarbonate kinetics parameters should be determined immediately before nutrient oxidation measurements to minimize possible day-to-day variations (20). Such determinations, however, require several hours when carried out with conventional bolus or primed constant-infusion techniques, and these procedures leave residual ^{13}C enrichment that may interfere with subsequent studies with ^{13}C-labeled nutrients. The bicarbonate model described in this study can be used to design and simulate primed variable-rate infusion protocols that should reduce markedly the duration of bicarbonate determinations as well as predict the behavior of residual ^{13}C.

The authors thank C. Garza for assistance in recruitment of subjects, L. Lee and M. Cabrera for expert analytical support, and E. R. Klein and M. Boyd for editorial work in preparation of this manuscript.

This work was supported by National Institutes of Health Grant AM-28129 and Grant RR-00188 from the General Clinical Research Centers Branch, and by USDA/ARS Children's Nutrition Research Center, Dept. of Pediatrics, Baylor College of Medicine and Texas Children's Hospital.

Received 21 October 1982; accepted in final form 11 March 1983.

APPENDIX

TABLE A1. *DOB values for each of 3 trials in 5 subjects vs. time after bolus NaH$^{13}CO_3$ injection*

Min	*Subj 1*			*Subj 2*			*Subj 3*			*Subj 4*			*Subj 5*		
	A	*B*	*C*	*A*	*B*	*C*	*A*	*B*	*C*	*A*	*B*	*C*	*A*	*B*	*C*
−30	0.1	−0.2	−0.3	−0.1	−0.1	0	−0.1	0	−0.2	0	0.3	−0.1	−0.1	0	0
−15	−0.1	0.2	0.3	0.1	0.1	0	0.1	0	0.2	−0.1	−0.3	0.1	0.1	0	0.4
0	−0.2	0.1	0.2	1.5	1.4	0.4	0.1	0.1	0	0	0.5	0	0.5	−0.2	−0.4
1	170.2	216.2	362.9	160.4	197.5	222.1	204.1	136.5	208.3	176.2	155.6	157.1	175.3	163.8	198.0
3	126.5	143.7	126.6	123.5	131.0	141.7	138.6	116.9	133.9	106.7	127.4	118.3	118.9	126.2	127.4
5	114.5	87.1	104.6	73.9	88.9	99.8	101.5	79.7	98.4	80.1	70.6	82.8	96.0	90.1	94.8
7	85.2	70.8	88.0	88.5	68.6	80.9	80.4	61.2	82.3	64.6	58.6	69.4	77.1	73.8	77.9
9	80.8	60.5	72.0	81.1	56.6	67.2	66.8	34.4	68.0	55.8	49.1	64.6	65.9	63.3	65.7
12	57.0	51.6	76.6	57.6	46.8	56.5	64.4	47.6	57.4	46.8	42.4	54.6	52.9	51.2	54.4
15	50.6	46.3	56.3	50.2	40.9	47.9	51.5	41.9	49.6	41.1	32.3	47.1	45.8	45.1	47.2
20	39.6	38.8	42.8	42.5	33.8	36.4	41.8	35.0	41.5	34.6	25.2	36.5	37.3	34.9	38.8
30	30.8	30.0	28.5	31.7	23.8	26.8	32.3	28.5	31.2	26.8	19.7	28.2	27.1	27.5	26.8
45	23.4	21.8	21.4	22.4	17.6	19.9	23.6	21.5	24.3	18.8	14.5	22.0	18.4	20.7	19.4
60	13.4	17.9	18.4	17.2	13.4	14.7	17.6	17.4	19.4	14.9	11.0	17.1	14.6	15.4	15.6
90	11.8	12.6	13.6	12.0	7.9	9.7	11.7	12.5	13.7	10.3	8.1	12.7	10.4	10.3	11.4
120	8.7	9.1	9.9	7.2	6.1	9.7	8.9	8.8	10.6	7.8	5.4	9.6	6.2	7.6	8.8
150	6.6	6.9	7.4	4.7	3.9	4.7	6.5	6.2	7.4	5.2	5.1	7.6	4.4	5.7	7.0
180	4.8	4.9	5.3	3.5	2.7	4.9	5.0	5.0	5.5	3.8	2.9	5.6	3.1	4.6	5.0
240	2.1	2.4	2.5	1.3	1.4	3.4	2.6	2.8	3.2	2.9	2.5	3.5	1.7	3.6	3.3
300	1.1	0.9	1.1	0.6	0.7	1.5	1.4	2.3	1.9	1.8	2.3	2.2	0.3	3.0	2.5
360	0.2	1.0	0.2	0.1	0.2	0.9	0.3	1.8	1.3	1.0		1.4	0.0	2.7	2.2

A–C, trials. DOB, incremental changes in ^{13}C abundance over base line.

REFERENCES

1. ALLSOP, J. R., R. R. WOLFE, AND J. F. BURKE. Tracer priming the bicarbonate pool. *J. Appl. Physiol.: Respirat. Environ. Exercise Physiol.* 45: 137–139, 1978.
2. ANNISON, E. F., R. E. BROWN, R. A. LENG, D. B. LINDSAY, AND C. E. WEST. Rates of entry and oxidation of acetate, glucose, D(−)-β-hydroxybutyrate, palmitate, oleate and stearate, and rates of production and oxidation of propionate and butyrate in fed and starved sheep. *Biochem. J.* 104: 135–147, 1967.
3. BAKER, N., W. W. SHREEVE, R. A. SHIPLEY, G. E. INCEFY, AND M. MILLER. C^{14} studied in carbohydrate metabolism. I. The oxidation of glucose in normal human subjects. *J. Biol. Chem.* 211: 575–592, 1954.
4. BERMAN, M., AND M. F. WEISS. *SAAM Manual.* Washington, DC: US DHEW, 1978, p. 78–180. (Publ. No. NIH 78-180)
5. BOYD, E. *The Growth of the Surface Area of the Human Body.* Minneapolis, MN: Univ. of Minnesota Press, 1935.
6. BROSNAN, J. T. Pathways of carbon flux in gluconeogenesis. *Federation Proc.* 41: 91–95, 1982.
7. CLAGUE, M. B., M. J. KEIR, AND P. D. WRIGHT. Development of a technique for measuring the oxidation rate of a ^{14}C-labelled substrate from $^{14}CO_2$ production without the need for collection of expired air. *Clin. Sci.* 60: 233–235, 1981.
8. COXON, R. V., AND R. J. ROBINSON. The transport of radioactive carbon dioxide in the blood stream of the dog after administration of radioactive bicarbonate. *J. Physiol. London* 147: 469–486, 1959.
9. COXON, R. V., AND R. J. ROBINSON. Movements of radioactive carbon dioxide within the animal body during oxidation of ^{14}C-labelled substances. *J. Physiol. London* 147: 487–510, 1959.
10. DRURY, D. R., A. N. WICK, AND M. C. ALMEN. Rate of elimination of labeled carbon dioxide from the body. *Am. J. Physiol.* 186: 361–364, 1956.
11. FARHI, L. E., AND H. RAHN. Dynamics of changes in carbon dioxide stores. *Anesthesiology* 21: 604–614, 1960.
12. FOWLE, A. S. E., C. M. E. MATTHEW, AND E. J. M. CAMPBELL. The rapid distribution of $^{3}H_2O$ and $^{11}CO_2$ in the body in relation to the immediate carbon dioxide storage capacity. *Clin. Sci.* 27: 51–

65, 1964.
13. GARLICK, P. J., AND G. A. CLUGSTON. Measurement of whole body protein turnover by constant infusion of carboxyl-labelled leucine. In: *Nitrogen Metabolism in Man*, edited by J. C. Waterlow and J. M. L. Stephen. Englewood, NJ: Applied Science, 1972, p. 303–322.
14. ISSEKUTZ, B., JR., P. PAUL, H. I. MILLER, AND W. M. BORTZ. Oxidation of plasma FFA in lean and obese humans. *Metabolism* 17: 62–73, 1968.
15. JAMES, W. P. T., P. J. GARLICK, P. M. SENDER, AND J. C. WATERLOW. Studies of amino acid and protein metabolism in normal man with L-[U-^{14}C]tyrosine. *Clin. Sci. Mol. Med.* 50: 525–532, 1976.
16. KORNBERG, H. L., R. E. DAVIEW, AND D. R. WOOD. The metabolism of ^{14}C-labelled bicarbonate in the cat. *Biochemistry* 51: 351–357, 1952.
17. LONG, C. L., J. L. SPENCER, J. M. KINNEY, AND J. W. GEIGER. Carbohydrate metabolism in normal man and effect of glucose infusion. *J. Appl. Physiol.* 31: 102–109, 1971.
18. MALMENDIER, C. L., C. DELCROIX, AND M. BERMAN. Interrelations in the oxidative metabolism of free fatty acids, glucose, and glycerol in normal and hyperlipemic patients. *J. Clin. Invest.* 54: 461–476, 1974.
19. MANOUGIAN, E., M. POLLYCOVE, J. A. LINFOOT, AND J. H. LAWRENCE. C^{14} glucose kinetic studies in normal, diabetic, and acromegalic subjects. *J. Nucl. Med.* 5: 763–895, 1964.
20. MATTHEWS, D. E., K. J. MOTIL, D. K. ROHRBAUGH, J. F. BURKE, V. R. YOUNG, AND D. M. BIER. Measurement of leucine metabolism in man from a primed, continuous infusion of L-[1-^{13}C]leucine. *Am. J. Physiol.* 238 (*Endocrinol. Metab.* 1): E473–E479, 1980.
21. MILLER, H., B. ISSEKUTZ, AND K. RODAHL. Effect of exercise on the metabolism of fatty acids in the dog. *Am. J. Physiol.* 205: 167–172, 1963.
22. MOOK, W. A., AND P. M. GROOTES. The measuring procedures and corrections for high precision mass spectrometric analysis of isotopic abundances ratio, especially referring to carbon, oxygen and nitrogen. *Int. J. Mass Spectrom. Ion Phys.* 12: 272, 1973.
23. MORRIS, B., AND M. W. MORGAN-SIMPSON. The excretion of $^{14}CO_2$ during the continuous intravenous infusion of $NaH^{14}CO_3$ in unanaesthetized rats. *J. Physiol. London* 169: 713–728, 1963.
24. MOTIL, K. J., D. M. BIER, D. E. MATTHEWS, J. F. BURKE, AND V. R. YOUNG. Whole body leucine and lysine metabolism studied with [1-^{13}C]leucine and [α-^{15}N]lysine: response in healthy young men given excess energy intake. *Metabolism* 30: 783–791, 1981.
25. MOTIL, K. J., D. E. MATTHEWS, D. M. BIER, J. F. BURKE, H. N. MUNRO, AND V. R. YOUNG. Whole body leucine and lysine metabolism: response to dietary protein intake in young men. *Am. J. Physiol.* 240 (*Endocrinol. Metab.* 3): E712–E721, 1981.
26. POYART, C. F., A. FREMINET, AND E. BURSAUX. The exchange of bone CO_2 in vivo. *Respir. Physiol.* 25: 101–107, 1975.
27. SCHOELLER, D. A., J. F. SCHNEIDER, N. W. SOLOMONS, J. B. WATKINS, AND P. D. KLEIN. Clinical diagnosis with the stable isotope ^{13}C in CO_2 breath test: methodology and fundamental considerations. *J. Lab. Clin. Med.* 90: 412–421, 1977.
28. SCHOELLER, D. A., AND P. D. KLEIN. A microprocessor-controlled mass spectrometer for the fully automated purification and isotopic analysis of breath CO_2. *Biomed. Mass Spectrom.* 6: 350–355, 1979.
29. SCHOELLER, D. A., P. D. KLEIN, J. B. WATKINS, T. HEIM, AND W. C. MACLEAN, JR. ^{13}C abundances of nutrients and the effect of variations in ^{13}C isotopic abundances of test meals formulated for $^{13}CO_2$ breath tests. *Am. J. Clin. Nutr.* 33: 2375–2385, 1980.
30. SEGAL, S., M. BERMAN, AND A. BLAIR. The metabolism of variously C^{14}-labeled glucose in man and an estimation of the extent of glucose metabolism by the hexose monophosphate pathway. *J. Clin. Invest.* 40: 1263–1279, 1961.
31. SHIPLEY, R. A., N. BAKER, G. E. INCEFY, AND R. E. CLARK. C^{14} studies in carbohydrate metabolism. IV. Characteristics of bicarbonate pool system in the rat. *Am. J. Physiol.* 197: 41–46, 1959.
32. SLANGER, B. H., N. KUSUBOV, AND H. S. WINCHELL. Effect of exercise on human CO_2-HCO_3^- kinetics. *J. Nucl. Med.* 11: 716–718, 1970.
33. SNEDECOR, G. W., AND W. G. COCHRAN. *Statistical Methods.* Ames, IA: Iowa State Univ. Press, 1967, p. 279–282.
34. STEELE, R. The retention of metabolic radioactive carbonate. *Biochem. J.* 60: 447–453, 1955.
35. WATERHOUSE, C., N. BAKER, AND H. ROSTAMI. Effect of glucose ingestion on the metabolism of free fatty acids in human subjects. *J. Lipid Res.* 10: 487–494, 1969.
36. WINCHELL, H. S., H. STAHELIN, N. KUSUBOV, B. SLANGER, M. FISH, M. POLLYCOVE, AND J. H. LAWRENCE. Kinetics of CO_2-HCO_3^- in normal adult males. *J. Nucl. Med.* 11: 711–715, 1970.
37. WOLFE, R. R., AND J. F. BURKE. Effect of burn trauma on glucose turnover, oxidation and recycling in guinea pigs. *Am. J. Physiol.* 233 (*Endocrinol. Metab.* 2): E80–E85, 1977.